Dalton Transactions

Accepted Manuscript

ROYAL SOCIETY OF CHEMISTRY

www.rsc.org/dalton

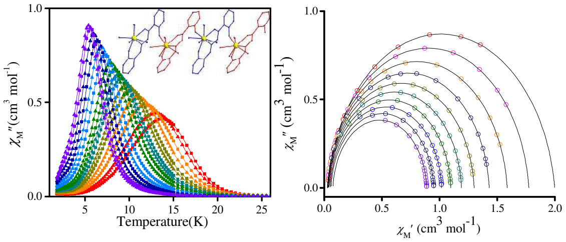

The one-dimensional Dy coordination polymer displays single-ion magnet behaviour with a narrow distribution of relaxation under a dc field.

Journal Name RSCPublishing

ARTICLE

Cite this: DOI: 10.1039/x0xx00000x

One-dimensional lanthanide coordination polymers: synthesis, structures, and single-ion magnetic behaviour

Hung-Kai Feng, Po-Jung Huang and Hui-Lien Tsai*

Received 00th January 2012,
Accepted 00th January 2012

DOI: 10.1039/x0xx00000x

www.rsc.org/

A family of isostructural one-dimensional (1D) lanthanide compounds with the formula $[Ln^{III}(L)(NO_3)(DMF)_2]_\infty$, where Ln = Tb (**1**), Dy (**2**), Ho (**3**) and Er (**4**) were synthesised, and structurally characterised. The magnetic behaviour of these compounds is demonstrated, and their static and dynamic properties are discussed and analyzed. The results of dc magnetic susceptibility measurements regarding compounds **1**–**4** indicate the existence thermal depopulation of the crystal field-induced splitting of m_J levels of Ln ions, while the observed frequency-dependent out-of-phase ac magnetic susceptibility signals under certain magnetic field for compounds **1**, **2**, and **4** show a slow relaxation of the magnetisation with an energy barrier of 6.15, 54.45, and 28.14 K, respectively. Also, complex **2** shows peak maxima of χ_M'' signals in temperature-dependent as well as frequency-dependent ac magnetic susceptibility measurements under a proper magnetic field, indicating that the relaxation process is dominantly thermally activated.

Introduction

The design and synthesis of materials that contain paramagnetic metal ions, such as lanthanide ions, with one- to three- dimensional functional coordination polymers, have attracted interest because their compelling network structures give rise to practical applications in diverse domains.[1–5] In recent decades, low-dimensional magnets, such as single-molecule magnets (SMMs)[6] and single-chain magnets (SCMs)[7] have intrigued physicists as well as chemists on account of their slow magnetic relaxation. The numerous attractive features of low-dimensional magnets such as quantum tunnelling magnetisation and magnetic hysteresis behaviour have been ascribed to this sort of magnetic behaviour.[8–9] Lanthanide ions, such as dysprosium(III) or terbium(III), possess an extremely large anisotropy with their high-magnitude quantum number ($\pm m_J$) and a pair of doubly degenerate ground states far separated from the first excited states, making them exceptionally appealing for being a SMM.

The fabrication and characterisation of polynuclear Ln compounds with interesting magnetic properties are thus of interest. However, the conditions that are required to produce anisotropy or zero-field splitting (ZFS) properties for such compounds are not clearly known.[10] Consequently, SMMs that contain a single spin carrier, namely a single-ion magnet (SIM), are attractive due to the simplification in the analysis of local anisotropy and ZFS.[11]

SIMs possess the magnetic anisotropy and their slow relaxation originates from the interaction between a single metal centre and its ligand field, which generates a large preferential orientation of the magnetic moment.[12] Ishikawa *et al.* first reported that phthalocyaninato lanthanide complexes with a single lanthanide centre exhibit slow relaxation of magnetisation.[13] Similarly, a number of mononuclear Tb(III), Dy(III), Ho(III), and Er(III) complexes have also been shown to display slow relaxation behaviour.[14]

To date, a number of lanthanide SIMs with slow relaxation behaviours have been synthesised based on diverse ligands, such as carboxylates,[15] β-diketonates,[11,16–20] macro-cyles,[21–23] and Schiff bases.[24–26] However, In contrast to the multi-nuclear lanthanide SMMs and lanthanide SIMs, 1D lanthanide

---

Department of Chemistry, National Cheng Kung University, Tainan 701, Taiwan, ROC.
Corresponding author. Tel.: +886 6 275 7575 65349; fax: +886 6 274 0552.
E-mail address: hltsai@mail.ncku.edu.tw (H.-L. Tsai).

Electronic supplementary information (ESI) available: The additional figures and tables. CCDC 1009151 (**2**), 1009152 (**4**), 1009153 (**3**), and 1009154 (**1**).

compounds show SMM properties are still rare, thus inspiring our group to further explore this type of compound.

In this paper, we report four compounds based on the Schiff base ligand of N-salicylidenesalicylhydrazide (H_2L), $[Ln^{III}(L)(NO_3)(DMF)_2]_\infty$, where Ln = Tb, Dy, Ho, or Er. Characterisation with single-crystal X-ray diffraction, powder X-ray diffraction, and elemental analyses were conducted. Experimental results reveal that the slow relaxation of magnetisation may be attributed to the SIM behaviour of Ln^{III} centre.

Experimental section

All solvents and reagents were used as received. The Schiff base ligand H_2L was obtained through the condensation of salicylhydrazide and salicylic aldehyde *in situ* (Scheme 1).

Syntheses of the complexes $[Ln^{III}(L)(NO_3)(DMF)_2]_\infty$, $[Ln^{III}$ = Tb (1), Dy (2), Ho (3), Er (4)]

Compound **1** was prepared by following the detail as shown below. $Tb(NO_3)_3{\cdot}5H_2O$ (0.5 mmol) was dissolved in DMF (20.0mL) and then a mixture of salicylhydrazide (0.5 mmol) and salicylic aldehyde (0.5 mmol) and Et_3N (1 mmol) were added. The bright-yellow solution was stirred for 0.5 h and then filtered. The resulting solution was treated with ether diffusion at room temperature for 4 days; yellow crystals formed. The yield was 26%. Anal. Calcd for $C_{20}H_{25}TbN_5O_{8.5}$ (corresponds to the absorption of half H_2O per molecule during the delivery of the sample to the elemental analysis instrument): C, 38.16; N, 11.13; H, 3.84. Found: C, 38.03; N, 11.38; H, 4.09%. IR data (KBr pellet cm^{-1}): 3448 (br), 1676 (s), 1655 (s), 1610 (s), 1581 (m), 1540 (w), 1523 (w), 1501 (w), 1467 (s), 1440 (s), 1301 (s), 1253 (m), 1151 (m), 769 (m).

Compound **2** was synthesised similar to **1**, but using $Dy(NO_3)_3{\cdot}6H_2O$ (0.5 mmol) instead of $Tb(NO_3)_3{\cdot}5H_2O$. Yellow crystals were also obtained with the yield of 19%. Anal. Calcd for $C_{20}H_{24}DyN_5O_8$: C, 38.40; N, 11.20; H, 3.84. Found: C, 38.10; N, 11.27; H, 4.05%. IR data (KBr pellet cm^{-1}): 3454 (br), 1676 (s), 1656 (s), 1610 (s), 1581 (m), 1541 (w), 1523 (w), 1501 (w), 1468 (s), 1440 (s), 1302 (s), 1152 (m), 770 (m).

Compound **3** was synthesised similar to **1**, but using $Ho(NO_3)_3{\cdot}5H_2O$ (0.5 mmol) instead of $Tb(NO_3)_3{\cdot}5H_2O$. Yellow crystals were formed with the yield of 33%. Anal. Calcd for $C_{20}H_{24}HoN_5O_8$: C, 38.29; N, 11.16; H, 3.86%. Found: C, 38.08; N, 11.38; H, 4.11%. IR data (KBr pellet cm^{-1}): 3448 (br), 1676 (s), 1655 (s), 1609 (s), 1580 (m), 1541 (w), 1500 (w), 1467 (s), 1440 (s), 1384 (s), 1301 (s), 1254 (w), 1152 (s), 770 (s).

Compound **4** was synthesised similar to **1**, but using $Er(NO_3)_3{\cdot}5H_2O$ (0.5 mmol) instead of $Tb(NO_3)_3{\cdot}5H_2O$. Yellow crystals were obtained with the yield of 28%. Anal. Calcd for $C_{20}H_{24}ErN_5O_8$: C, 38.11%; N, 11.12; H, 3.81. Found: C, 37.91; N, 11.21; H, 3.93%. IR data (KBr pellet cm^{-1}): 3448 (br), 1676 (s), 1656 (s), 1610 (s), 1581 (m), 1541 (s), 1523 (s), 1500 (w), 1467 (s), 1348 (w), 1305 (s), 1151 (m), 769 (m).

Physical measurements

Infrared spectra were recorded in the solid state (KBr pellet) on a Nicolet 380 FTIR spectrometer in the 4000–400 cm^{-1} range. The elemental analysis for C, H, and N was carried out with an Elementar Vario EL III analyzer. Variable-temperature dc magnetic susceptibility measurements and ac magnetic susceptibility measurements were conducted on microcrystalline samples, suspended in eicosane to prevent torquing. Variable-temperature dc magnetic susceptibility measurements for **1–4** were performed on a Quantum Design MPMS7 magnetometer equipped with a 7.0 T magnet, operating in the range of 2.0-300.0 K. Reduced magnetisation measurements for complexes **1–4** were carried out on a Quantum Design MPMS SQUID VSM magnetometer in ranges 0–70 kOe and 2.0–4.0 K. Ac magnetic susceptibility measurements were carried out on Quantum Design PPMS-9 magnetometer equipped with a 9.0 T magnet and operating in the range of 1.8–300K. Diamagnetic corrections were estimated from Pascal′s constant and subtracted from the experimental susceptibility data to determine the molar paramagnetic susceptibility of the compound.[27] X-ray powder diffraction was measured using a Shimadzu XRD-7000S X-ray diffractometer with Cu K_α radiation (λ = 1.54060 Å).

X-ray crystallography

The data collection parameters for complexes **1–4** are listed in Table 1. Diffraction measurements for complexes **1–4** were carried out using a Bruker SMART APEX II CCD diffractometer with graphite-mono-chromated Mo K_α radiation (λ = 0.71073 Å). Cell parameters were retrieved and refined using the Bruker SAINT software package for all reflections. Data reduction was also performed with this software. The structure was solved using the direct method and refined using the SHELXL-97 program with full-matrix least-squares on F^2 values.[28] All non-hydrogen atoms were refined anisotropically, whereas hydrogen atoms were placed in ideal, calculated positions, with isotropic thermal parameters riding on their respective carbon and oxygen atoms.

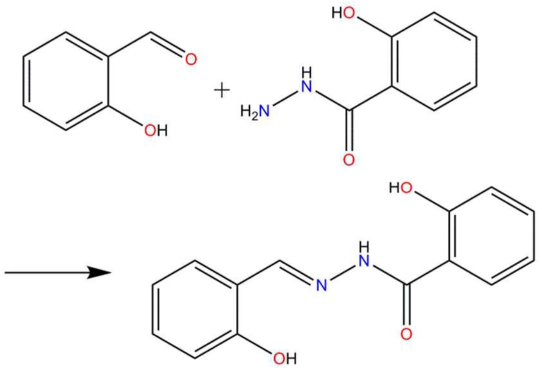

Scheme 1. Synthesis of H_2L

Table. 1 The crystallographic data and collection parameters for complexes **1**–**4**.

	1	**2**	**3**	**4**
Formula	$C_{20}H_{24}TbN_5O_8$	$C_{20}H_{24}DyN_5O_8$	$C_{20}H_{24}HoN_5O_8$	$C_{20}H_{24}ErN_5O_8$
Formula weight	621.36	624.94	627.37	629.70
Crystal system	Orthorhombic	Orthorhombic	Orthorhombic	Orthorhombic
Space group	*P*bca	*P*bca	*P*bca	*P*bca
a (Å)	17.5789(15)	17.5564(10)	17.497(2)	17.4707(14)
b (Å)	10.6997(9)	10.6174(6)	10.6651(12)	10.7118(9)
c (Å)	25.330(2)	25.2308(14)	25.333(3)	25.398(2)
V (Å^3)	4764.3(7)	4703.1(5)	4727.4(9)	4753.1(7)
Z	8	8	8	8
T (K)	150(2)	150(2)	150(2)	150(2)
D_{calc} (g/cm^3)	1.733	1.765	1.763	1.760
μ (mm^{-1})	3.023	3.232	3.402	3.586
Reflections collected	33893	37616	34501	18338
Data/restraints/parameters	5908 / 1 / 311	6584 / 1 / 311	5867 / 1 / 311	2646 / 0 / 293
R(int)	0.0441	0.0321	0.0492	0.0339
Goodness-of-fit on F^2	1.029	1.027	1.029	1.117
Max. and min. transmission	0.7457, 0.6589	0.7459, 0.6024	0.7457, 0.5914	0.7446, 0.6281
$R_1{}^a$, $wR_2{}^b$ [$I > 2\sigma(I)$]	0.0295, 0.0640	0.0252, 0.0615	0.0310, 0.0612	0.0347, 0.0718
$R_1{}^a$, $wR_2{}^b$ (all data)	0.0525, 0.0731	0.0347, 0.0665	0.0539, 0.0690	0.0425, 0.0760
Largest diff. peak and hole (e Å^{-3})	1.027 and −0.741	1.803 and −0.531	1.186 and −0.670	1.439 and −1.425

$^aR_1 = (\Sigma||F_0| - |F_c||) / \Sigma|F_0|$ $^bwR_2=[\Sigma[w(F_0{}^2-F_c{}^2)^2 / \Sigma [w(F_0{}^2)^2]]^{1/2}$

Results and discussion

Syntheses

This study synthesised a family of materials employing lanthanide ions with different anisotropies. At first, we synthesised dysprosium-base compound, but to check if structural changes took place with elements before or after Dy in periodic table, we tried to synthesise with different lanthanide ions. However, we could synthesise only compounds with Tb, Ho, Er, finding that they are isostructural.

The reaction of $Ln(NO_3)_3·xH_2O$, where Ln = Tb, Dy, Ho or Er, with salicylhydrazide and salicylic aldehyde lead to the development of a bright-yellow reaction mixture.

The resulting mixture was stirred at room temperature for 0.5 h and then filtered. The residue was slowly diffused with Et_2O to produce yellow crystals of $[Ln^{III}(L)(NO_3)(DMF)_2]_\infty$ (Ln = Tb, Dy, Ho or Er) with yields of 26.2%, 18.7%, 33.2%, and 27.9% for **1**, **2**, **3**, and **4**, respectively. The original expectation of the system of reaction was a product of merely pure SMM, however, the final product was a zigzag 1D lanthanide mononuclear single-molecule magnet because of the anti-bridge mode of L ligand between Ln ions

To confirm that these lanthanide complexes were isostructural, powder diffraction patterns were recorded for all complexes. The X-ray powder diffraction patterns of **1**–**4** are consistent with data simulated based on CIF files for corresponding compounds (Fig. S1), thus confirming the purity of the bulk samples.

Description of structures

Single-crystal X-ray diffraction analyses reveal that complexes **1**–**4** are isostructural. Selected interatomic distances and angles are listed in Table S1. Below, the structure of complex **2** is briefly described. Complex **2** crystallises in the orthorhombic space group *P*bca.

As shown in Fig. 1 (a), the ORTEP representation of **2** has one independent Dy atom in the asymmetric unit. The peripheral ligands in complex **2** are provided by two DMF molecules, one nitrate group, and one doubly deprotonated H_2L ligand. In addition, the doubly deprotonated H_2L ligand behaves as a $\eta^1:\eta^1:\eta^1:\eta^1:\mu_2$ ligand, bridging two Dy^{III} ions through phenoxido group O3, O1, O2, and N1. The nitrate group in complex **2** adopts a bidentate mode with Dy. Furthermore, each DMF molecule is terminally coordinated to Dy. All coordination modes of the ligands of complex **2** are labelled in Scheme 2.

Here, the eight-coordinate Dy centre displays the distorted dodecahedral coordination geometry shown in Fig. 1 (c). Along the *b* crystallographic axis, as shown in Fig. 1 (b) and (d), the Dy^{III} ions are connected by an L ligand to create the 1D zigzag chain of $[Dy^{III}(L)(NO_3)(DMF)_2]_\infty$, where the closest Dy···Dy distance is ca. 7.536 Å. The Dy^{III} centres can thus be considered to be isolated from a magnetic point of view. Moreover, the Ln-O distances are in the range of 2.188(3)–2.497(2), 2.178(2)–2.491(2), 2.175(3)–2.472(3), 2.163(5)–2.465(5) Å, the Ln-N distances are 2.559(3), 2.545(2), 2.536(3), and 2.508(5) Å, and the Ln···Ln distances are 7.574, 7.536, 7.518, and 7.487 Å for complexes **1**, **2**, **3**, and **4**, respectively. The Ln-O, Ln-N and Ln···Ln distances follow the trend of lanthanide contraction and decrease from the following series: Tb, Dy, Ho, and Er for complexes **1**, **2**, **3**, and **4**, respectively.

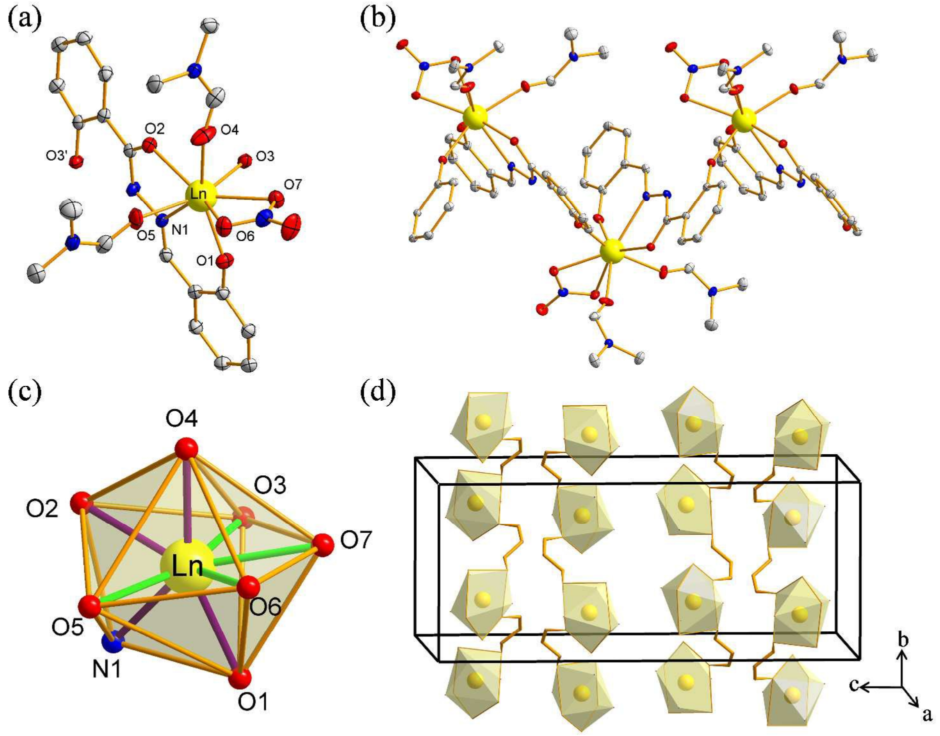

Fig. 1 (a) Asymmetric unit of complexes **1**–**4**. H atoms have been omitted for clarity. (b) 1D linkage mode in complexes **1**–**4**. H atoms are omitted for clarity. (Ln: bright yellow, O: red, N: blue, C: grey). (c) View of coordination environments around Ln centre as distorted dodecahedral geometry for **1**–**4**. (d) Perspective view of Ln chain of **1**–**4** together with unit cell along *b* axis.

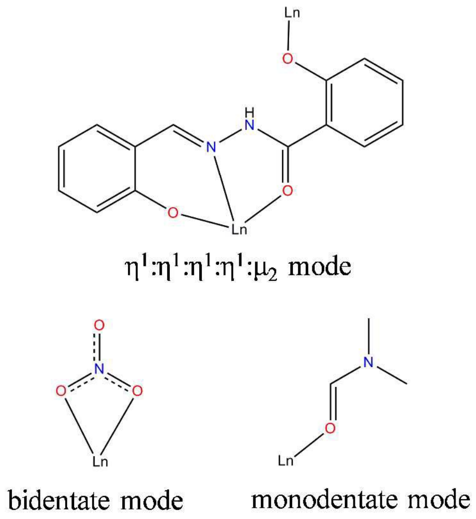

Scheme 2. Coordination modes of H_2L, nitrate and DMF groups within complexes **1**–**4**.

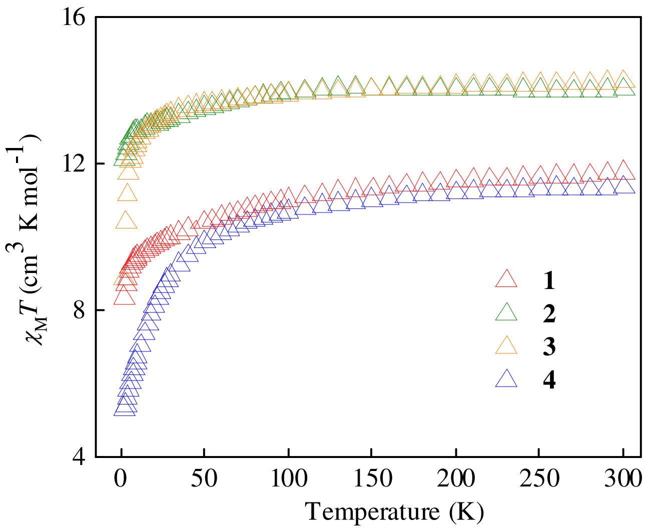

Fig. 2 Plot of $\chi_M T$ versus temperature for complexes **1**–**4**.

Magnetic properties

The dc magnetic susceptibility measurements of complexes **1**–**4** (Fig. 2) were conducted in the temperature range of 2–300 K with an applied magnetic field of 1000 Oe. The room-temperature $\chi_M T$ values of 11.78, 14.04, 14.23, 11.37 and cm^3 K mol^{-1}, are in agreement with the expected values of 11.81, 14.17, 14.06, and 11.48 cm^3 K mol^{-1} for complexes **1**, **2**, **3**, and **4**, respectively. The $\chi_M T$ value for complex **2** decreased tardily upon cooling from 300 to 30 K, and then dropped drastically to a minimum value of 12.10 cm^3 K mol^{-1} at 2 K. The $\chi_M T$ values for complexes **1**, **3**, and **4** show similar behaviours to that of those for complex **2**, decreasing slightly with decreasing temperature, from 300 K to 10, 20, and 50 K, and then dropping rapidly to 8.35, 8.87, and 5.32 cm^3 K mol^{-1} at 2 K, respectively. The decrease of $\chi_M T$ with decreasing temperature can be most properly explained by the thermal depopulation of the excited crystal field-induced splitting m$_J$ levels of Ln^{III} ions.[29–30]

Magnetisation data for complex **2** were collected in the ranges of 0.1–70 kOe and 2.0–4.0 K. The results for complex **2** are plotted as reduced magnetisation M versus H/T in Fig. S2. The magnetisation increases rapidly below 10 kOe and then more gradually increase with saturation at fields higher than 20 kOe, reaching 4.60 Nβ at 2 K under 70 kOe. This value is much lower than the expected saturation value of 10 Nβ (10 Nβ for each Dy^{III} ion), which can be attributed to the crystal field-induced splitting of the m$_J$ level together with magnetic anisotropy. In addition, the value is also lower than the hypothetic value of 5.23 Nβ for one uncorrelated Dy^{III} ion by virtue of the entirely different coordination environment since the magnetic properties of lanthanide-based complexes are quiet sensitive to the crystal field around a single lanthanide ion.[31] The magnetisation for complex **1** reaches 5.30 Nβ with an approximate saturation at 2 K under 70 kOe, which is still much lower than the expected saturation value of 9 Nβ (9 Nβ for each Tb^{III} ion). This result can be attributed to the same explanation as that for complex **2**. The magnetisations for complexes **3** and **4** display a similar sharp increase at 2 K under low fields (Figs. S3, S4, and S5). Under fields above 10 kOe, the magnetisations for complexes **3** and **4** increase linearly, reaching ca. 5.47 and 4.86 Nβ, respectively, without clear saturation. These maximum values are lower than theoretical saturation values of 10 Nβ for Ho^{III} ion and 9 Nβ for Er^{III} ion, which is also attributed to ligand-field-induced splitting. Furthermore, the non-superposition of M versus H/T isothermal curves shown in Figs. S3, S4, and S5 demonstrate the presence of magnetic anisotropy and/or low-lying excited states in complexes **1**, **3**, and **4**.

Measurements of ac magnetic susceptibility were performed on microcrystalline samples for complexes **1**–**4** in the temperature range of 1.8–25 K under a zero dc field and a 3.5 Oe ac field and with an applied static field oscillating in the frequency range of 100–10000 Hz. For complex **2**, the in-phase $\chi_M'T$ and out-of-phase χ_M'' versus T plots under a zero-dc field are shown in Fig. 3 (left). The out-of-phase χ_M'' signals for complex **2** appear below 20 K, revealing the onset of slow magnetisation relaxations. Nevertheless, the peak maxima of the χ_M'' signals are not observed at temperatures above 1.8 K but weak broad shoulders are observed instead due to the fast quantum tunnelling relaxation, a phenomenon that is usually found for other SIMs.[32–33] Therefore, the relaxation time (τ_0) and energy barrier (U_{eff}) cannot be determined via the Arrhenius law and fitting the data into a Debye model was not successful (Fig. S6).[34–37] From the temperature dependence of ac magnetic susceptibilities, when an adequate field (e.g., 3000 Oe) is applied, well-shape peak-like curves are obtained and strong frequency-dependent maxima are observed below ca. 16 K for both χ_M' and χ_M'', as shown in Fig. 3 (right). Moreover, the out-of-phase χ_M'' signals shift to a lower temperature with decreasing frequency, indicating a thermally activated relaxation process. The optimal dc field of 3000 Oe was chosen by performing field-dependent measurements at 1.8 K and 10 K as shown in Figs. S7 and S8. The out-of-phase signals are suppressed to a significant extent under external dc fields, which is indicative of the quenching effect of the quantum tunnelling magnetisation (QTM). It also noteworthy that the signals in the low frequency range are enhanced with increasing field below 400 Oe, but then start to be suppressed under stronger fields and completely disappear above a field of 3000 Oe. However, distinct responses to the dc fields were observed at 10 K: the χ_M'' signals in the high frequency range are suppressed in weak dc fields but increase under condition of strong fields with a turning point of 3000 Oe, whereas the signals below 5000 Hz display an opposite response, reaching maxima near a 3000 Oe dc field. In order to obtain a pure thermally activated-type of relaxation process with narrow distribution of relaxation times, we chose a dc field of 3000 Oe based on the above results. From the frequency dependence of the ac magnetic susceptibilities under 3000 Oe dc field in the range of 4–14.5 K in Fig. 4 (top), the relaxation times (τ) were calculated from the frequencies ($\tau^{-1} = 2\pi\nu$) of the peak maxima at the corresponding temperatures (Table S2).

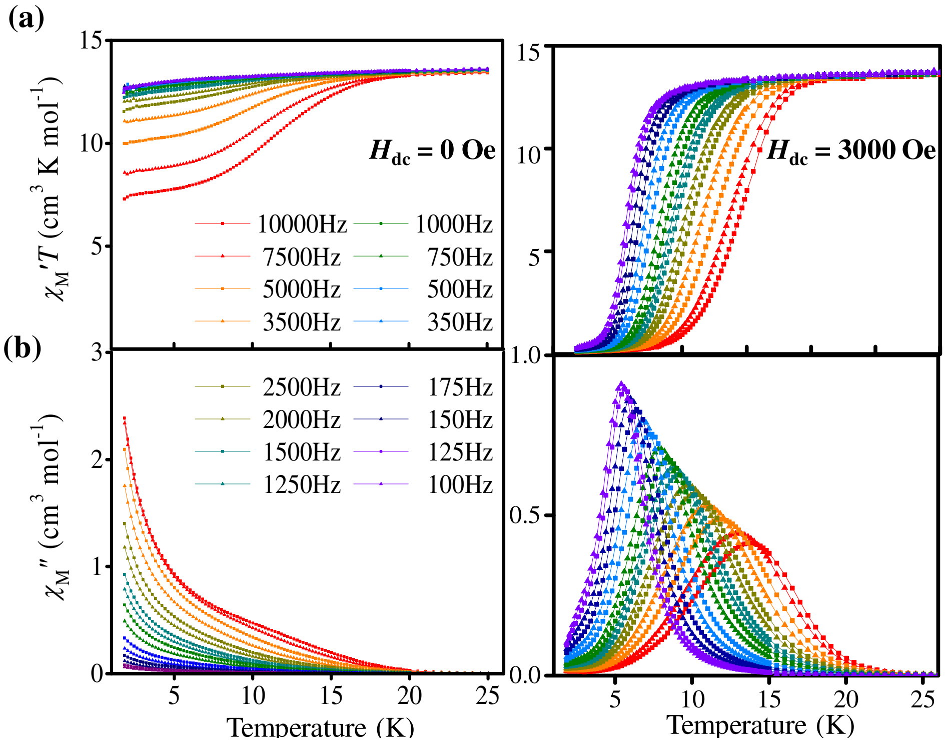

Fig. 3 (a) Plots of $\chi_M'T$ and (b) χ_M'' vs. temperature for a microcrystalline sample of complex **2** in (left) zero and (right) 3000 Oe dc field in a 3.5-Oe ac field. The data were collected in an ac field oscillating at the indicated frequency.

The ln(τ) versus T^{-1} plot is shown in Fig. S9. Above 7 K, the relaxation processes can be considered as being thermally activated. When fitted to the Arrhenius equation, they give anenergy barrier (U_{eff}) of 44.02 K with a characteristic time (τ_0) of 1.01 × 10^{-6} s, which is consistent with the expected τ_0 of 10^{-6}–10^{-11} for SMMs.[38] Below 8 K, the relaxation becomes slightly temperature-independent. This indicates that there are multiple relaxation processes at low temperature in this system. From the frequency dependence of ac magnetic susceptibilities under 3000 Oe dc field in the range of 6–15 K in Fig. 4 (bottom), Cole-Cole plots in the form of χ_M'' versus χ_M' exhibit a nearly semicircular form, which can be fitted to the generalised Debye model. The results of the α parameter and relaxation time τ from fitting are listed in Table S3. The values of α parameter suggest that the distribution of relaxation time is narrow. This result is in agreement with that of Arrhenius fitting above 8 K. Moreover, the relaxation times obtained from the fitting results of Cole-Cole analyses could br fitted into the Arrhenius law as well, resulting in a larger U_{eff} of 54.45 K and a faster τ_0 of 3.22 × 10^{-7} s as shown in Fig. S9.

Among this series of compounds, complexes **1**, **3**, and **4** show negligible out-of-phase signals without a static field, illustrating the absence of slow relaxation of magnetisation

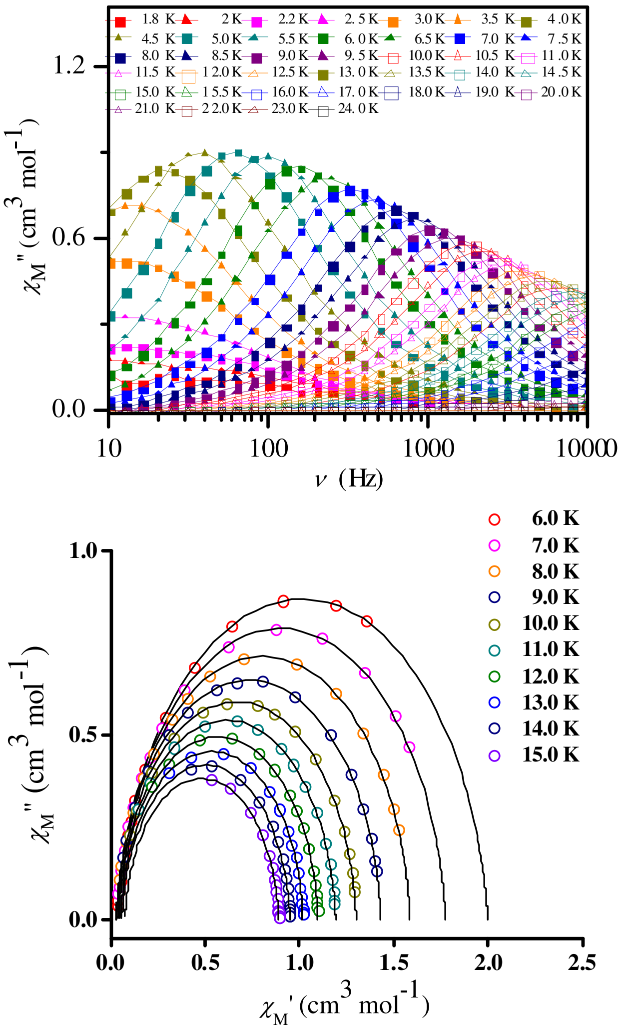

Fig. 4 (top) Plots of χ_M'' versus frequency for microcrystalline sample of complex **2** in 3000 dc field and 3.5-Oe ac field oscillating at the indicated temperature and (bottom) Cole–Cole plots of χ_M'' vs. χ_M' for complex **2** at 6.0-15.0 K under a 3000 Oe dc field. Solid lines are the best fits to experimental data using Debye model.

(Figs. S10–S12). However, complexes **1** and **4** display slow relaxation behaviour when a proper magnetic field is applied, whereas complex **3** still shows negligible out-of-phase signals (Figs. S13–S15). Therefore, the quantum tunnelling of magnetisation by Zeeman splitting of the degenerate states for complexes **1** and **4** were suppressed by the applied static magnetic field. Due to the differences in the electronic fine structure, these compounds display distinct dynamic magnetic properties. Similar to the measurements performed on complex **2**, field-dependent data for **1**, **3**, and **4** at 1.8 K were collected and analysed. The out-of-phase components in the high frequency range are enhanced under a stronger dc field, with maxima of 1000 and 1500 for **1** and **3**, respectively, which are the bias fields under which the QTM would be expected to be suppressed (Fig. S16). In the case of complex **4**, the determination is quite different, since temperature-dependent ac susceptibility measurements performed in 600 Oe fail to reach a maximum even at 1.8 K and in a 10000 Hz ac field. Thus, the optimal field selected for **4** was greater than 600 Oe, but before the signals are suppressed significantly, i.e. the dc field of 1000 Oe. For complex **1** measured in 1000 Oe bias field, maxima of χ_M'' can only be observed in high frequency at temperatures above 1.8 K, thus the U_{eff} cannot be determined by using the Arrhenius law. However, a method used by Bartolomé *et al.*,[39–40] assuming that the SMM relaxation has only a single characteristic relaxation process of the Debye type with merely one energy barrier and one relaxation time, can be employed to roughly calculate the relaxation time and energy barrier. As shown in Fig. S17, the fitting results over range 500–2500 Hz are more precise. Also, the estimation of both the activation energy of 6.15 K and the characteristic time of 9.75×10^{-6} s can be obtained based on the fitting of the experimental χ_M''/χ_M' data to the equation. From the temperature dependence of ac magnetic susceptibilities under 1000 Oe dc field, the energy barrier of 28.14 K with a characteristic time of 3.27×10^{-11} s were obtained from the fitting of the Arrhenius law in the range of 1.94–2.15 K for complex **4** (Fig. S18).

The slow magnetic relaxation found in this series of complexes can mainly be attributed to the magnetic anisotropy within a single lanthanide ion since the shortest Ln···Ln distances are in the range of 7.5–7.6 Å, which would prevent any possible exchange coupling between the spin carriers to occur, i.e. the presence of SIM behaviour but with one-dimensional structures. This phenomenon is still rare among the 1D lanthanide-based coordination polymers and thus provides a new strategy for the construction of a SIM by employing ligands with poly-O donor atoms that are far from one another, thus extending the distance between neighbouring Ln$^{\mathrm{III}}$ centres. In the case of complexes **1**–**4** is the Schiff base ligand H$_2$L which successfully isolates each lanthanide ion with its anti-bridging mode.

An investigation of the crystal field effect on magnetic anisotropy from the standpoint of the dynamic properties of three eight-coordinated mononuclear Dy$^{\mathrm{III}}$-based complexes with distinct coordination geometries was recently reported.[41] The three compounds possess distorted bicapped trigonal prismatic (BTP), dodecahedral (DD), and square antiprismatic (SAP) geometries, where only the last two compounds show SIM behaviour with the SAP complex exhibiting the highest anisotropy barrier. This result again confirms the importance of the coordination geometry around Dy$^{\mathrm{III}}$ ion and interestingly, reveals that a Dy$^{\mathrm{III}}$-based complex with a small nuclear number per molecule usually possesses a higher U_{eff} when the coordination topology or the structure is more symmetrical,[13,42] i.e. a proper crystal field effect on the Dy$^{\mathrm{III}}$ centre results in the ground states that are well-separated from the first excited states, that is, spin-axiality and magnetic anisotropy are improved.[14i,43] Complex **3** whose eight-coordinated Dy$^{\mathrm{III}}$ ion possesses a distorted dodecahedral geometry with a quasi-D$_{2d}$ symmetry shows slow relaxation with a moderate anisotropy barrier of 54.45 K. The value is smaller than the complexes with D$_{4d}$ and D$_{5h}$ symmetries by virtue of the weaker axiality of the D$_{2d}$ geometry.[13,14i]

Conclusion

A family of 1D complexes based on rare-earth elements was synthesised and characterised. All of the compounds contained the Schiff base of N-salicylidenesalicylhydrazide along with two DMF molecules and a nitrate group as ligands. Complexes **1**–**4** were isostructural, revealing trend of the lanthanide contraction. In terms of magnetic properties, dc magnetic susceptibility analyses of complexes **1**–**4** indicate the thermal depopulation of the excited degenerate m_J levels of these lanthanide ions. Complexes **1** and **4** exhibit field-induced slow magnetic relaxation, while complex **2** shows slow magnetic relaxation without applying dc field. Furthermore, complex **2** has peak maxima of χ_M'' signals in temperature dependence as well as frequency dependence of ac magnetic susceptibility measurements with an energy barrier of 54.45 K in the high-temperature region, indicating that the relaxation process is dominantly thermally activated. The values of the α parameter for nearly semicircular Cole-Cole plots increase with decreasing temperature, indicating that the distribution of relaxation time is narrow. Additionally, the energy barrier 6.15 and 28.15 K for complexes **1** and **4** were obtained from analyses of under-field ac magnetic susceptibilities. The anisotropy barriers in complexes **1**–**4** are not as prominent as would be expected due to the relative weaker spin axiality in the local D_{2d} symmetry of Ln^{III} centre, but the successful isolation of a single lanthanide ion still demonstrates that complexes **1**–**4** are viable compounds.

Acknowledgements

The authors acknowledge the Ministry of Science and Technology of the Republic of China for financially supporting this study under grant NSC 102-2113-M-006-006-MY2.

References

(1) (a) M. Eddaoudi, J. Kim, N. Rosi, D. Vodak, J. Wachter, M. O′Keeffe and O. M. Yaghi, *Science*, 2002, **295**, 469; (b) S. Kitagawa, R. Kitaura and S.-I. Noro, *Angew. Chem. Int. Ed.*, 2004, **43**, 2334; (c) G. Férey, C. Mellot-Draznieks, C. Serre and F. Millange, *Acc. Chem. Res.*, 2005, **38**, 217; (d) M. O′Keeffe, M. A. Peskov, S. J. Ramsden and O. M. Yaghi, *Acc. Chem. Res.*, 2008, **41**, 1782; (e) N. W. Ockwig, O. Delgado-Friedrichs, M. O′Keeffe and O. M. Yaghi, *Acc. Chem. Res.*, 2005, **38**, 176; (f) G. Férey, *Chem. Soc. Rev.*, 2008, **37**, 191; (g) S. Ma and H.-C. Zhou, *Chem. Commun.*, 2010, **46**, 44; (h) H.-L. Jiang and Q. Xu, *Chem. Commun.*, 2011, **47**, 3351.

(2) (a) D. W. Bruce and D. O′Hare, *Inorganic Materials*, John Wiley & Sons, New York, 1992; (b) R. D. Willet, D. Gatteschi and O. Kahn, *Magneto-structural Correlations in Exchange Coupled System*, NATO ATI Series C140, Reidal, Dordrecht, The Netherlands, 1985.

(3) (a) B. Multon and M. J. Zaworotko, *Chem. Rev.*, 2001, **101**, 1629; (b) P. J. Hagrman, D. Hagrman and J. Zubieta, *Angew. Chem. Int. Ed.*, 1999, **38**, 2638; (c) R. Robson, *J. Chem. Soc., Dalton Trans.*, 2000, 3735; (d) W. Su, M. Hong, J. Weng, R. Cao and S. Lu, *Angew. Chem. Int. Ed.*, 2000, **39**, 2911; (e) A. Saitoh, H. Miyasaka, M. Yamashita and R. Clérac, *J. Mater. Chem.*, 2007, **17**, 2002; (f) D. J. Collins and H.-C. Zhou, *J. Mater. Chem.*, 2007, **17**, 3154; (g) J. V. Barth, G. Costantini and K. Kern, *Nature*, 2005, **437**, 671; (h) A. Guijarro, O. Castillo, L. Welte, A. Calzolari, P. J. Sanz Miguel, C. J. Gómez-García, D. Olea, R. di Felice, J. Gómez-Herrero and F. Zamora, *Adv. Mater.*, 2010, **22**, 1451.

(4) (a) D. Gatteschi, O. Kahn and J. Miller, *Molecular Magnetic Materials*, Nato ASI Series EI98, Kluwer, Dordrecht, The Netherlands, 1991; (b) O. M. Yaghi, G. Li and H. Li, *Nature*, 1995, **378**, 703; (c) C. Chen and K. S. Suslick, *Coord. Chem. Rev.*, 1993, **128**, 293 and references cited therein.

(5) (a) M. Kondo, Y. Irie, Y. Shimizu, M. Miyazawa, H. Kawaguchi, A. Nakamura, T. Naito, K. Maeda and F. Uchida, *Inorg. Chem.*, 2004, **43**, 6139; (b) S. C. Johannessen and R. G. Brisbois, *J. Am. Chem. Soc.*, 2001, **123**, 3818; (c) U. Mueller, M. Schubert, F. Teich, H. Puetter, K. Schierle-Arndt and J. Pastré, *J. Mater. Chem.*, 2006, **16**, 626; (d) H. Iguchi, S. Takaishi and M. Yamashita, *Chem. Lett.*, 2014, **43**, 69; (e) S. Kumagai, S. Takaishi, B. K. Breedlove, H. Okamoto, H. Tanaka, S. Kuroda and M. Yamashita, *Chem. Commun.*, 2014, **50**, 8382.

(6) (a) D. N. Woodruff, R. E. P. Winpenny and R. A. Layfield, *Chem. Rev.*, 2013, **113**, 5110; (b) W. Wernsdorfer, N. Aliaga-Alcalde, D. N. Hendrickson and G. Christou, *Nature*, 2002, **416**, 406; (c) D. Gatteschi and R. Sessoli, *Angew. Chem. Int. Ed.*, 2003, **42**, 268; (d) A. J. Tasiopoulos, A. Vinslava, W. Wernsdorfer, K. A. Abboud and G. Christou, *Angew. Chem. Int. Ed.*, 2004, **43**, 2117; (e) Y. Song, P. Zhang, X.-M. Ren, X.-F. Shen, Y.-Z. Li and X.-Z. You, *J. Am. Chem. Soc.*, 2005, **127**, 3708; (f) G. Aromí and E. K. Brechin, *Struct. Bonding* (Berlin) 2006, **122**, 1 and references therein; (g) A. M. Ako, I. J. Hewitt, V. Mereacre, R. Clérac, W. Wernsdorfer, C. E. Anson and A. K. Powell, *Angew. Chem. Int. Ed.*, 2006, **45,** 4926; (h) E. J. Schelter, F. Karadas, C. Avendano, A. V. Prosvirin, W. Wernsdorfer and K. R. Dunbar, *J. Am. Chem. Soc.*, 2007, **129**, 8139; (i) H. L. C. Feltham and S. Brooker, *Coord. Chem. Rev.,* 2014, **276**, 1.

(7) (a) A. Caneschi, D. Gatteschi, N. Lalioti, C. Sangregorio, R. Sessoli, G. Venturi, A. Vindigni, A. Rettori, M. G. Pini and M. A. Novak, *Angew. Chem. Int. Ed.*, 2001, **40**, 1760; (b) R. Clérac, H. Miyasaka, M. Yamashita and C. Coulon, *J. Am. Chem. Soc.*, 2002, **124**, 12837; (c) R. Lescoëuzec, J. Vaissermann, C. Ruiz-Pérez, F. Lloret, R. Carrasco, M. Julve, M. Verdaguer, Y. Dromzee, D. Gatteschi and W. Wernsdorfer, *Angew. Chem. Int. Ed.*, 2003, **42**, 1483; (d) T.-F. Liu, D. Fu, S. Gao, Y.-Z. Zhang, H.-L. Sun, G. Su and Y.-J. Liu, *J. Am. Chem. Soc.*, 2003, **125**, 13976; (e) S. Wang, J.-L. Zuo, S. Gao, Y. Song, H.-C. Zhou, Y.-Z. Zhang and X.-Z. You, *J. Am. Chem. Soc.*, 2004, **126**, 8900; (f) Y.-L. Bai, J. Tao, W. Wernsdorfer, O. Sato, R.-B. Huang and L.-S. Zheng, *J. Am. Chem. Soc.*, 2006, **128**, 16428.

(8) (a) L. Thomas, F. Lionti, R. Ballou, D. Gatteschi, R. Sessoli and B. Barbara, *Nature*, 1996, **383**, 145; (b) J. R. Friedman, M. P. Sarachik, J. Tejada and R. Ziolo, *Phys. Rev. Lett.*, 1996, **76**, 3830.

(9) R. Sessoli, D. Gatteschi, A. Caneschi and M. A. Novak, *Nature*, 1993, **365**, 141.

(10) D. Gatteschi and L. Sorace, *J. Solid State Chem.*, 2001, **159**, 253.

(11) S.-D. Jiang, B.-W. Wang, G. Su, Z.-M. Wang and S. Gao, *Angew. Chem. Int. Ed.*, 2010, **49**, 7448 .

(12) J. D. Rinehart and J. R. Long, *J. Am. Chem. Soc.*, 2009, **131**, 12558.

(13) (a) N. Ishikawa, M. Sugita, T. Ishikawa, S. Koshihara and Y. Kaizu, *J. Am. Chem. Soc.*, 2003, **125**, 8694; (b) N. Ishikawa, M. Sugita and W. Wernsdorfer, *J. Am. Chem. Soc.*, 2005, **127**, 3650.

(14) (a) A. AlDamen, J. M. Clemente-Juan, E. Coronado, C. Marti-Gastaldo and A. Gaita-Arino, *J. Am. Chem. Soc.*, 2008, **130**, 8874; (b) A. Yamashita, A. Watanabe, S. Akine, T. Nabeshima, M. Nakano, T. Yamamura and T. Kajiwara, *Angew. Chem. Int. Ed.*, 2011, **50**, 4016; (c) H. L. C. Feltham, Y.-H. Lan, F. Klöwer, L. Ungur, L. F. Chibotaru, A. K. Powell and S. Brooker, *Chem.–Eur. J.*, 2011, **17**, 4362; (d) S.-D. Jiang, S.-S. Liu, L.-N. Zhou, B.-W. Wang, Z.-M. Wang and S. Gao, *Inorg. Chem.*, 2012, **51**, 3079; (e) K. R. Meihaus and J. R. Long, *J. Am. Chem. Soc.*, 2013, **135**, 17952; (f) J. J. Le Roy, I. Korobkov and M. Murugesu, *Chem. Commun.*, 2014, **50**, 1602; (g) Y.-N. Guo, L. Ungur, G. E. Granroth, A. K. Powell, C.-J. Wu, S. E. Nagler, J.-K. Tang, L. F. Chibotaru and D.-M. Cui, *Scientific Reports*, 2014, **4**, 5471; (h) P. Hu, Z. Sun, X.-F. Wang, L.-C. Li, S.-Z. Liao and D. Luneau, *New J. Chem.*, 2014, **38**, 4716; (i) J.-L. Liu, J.-Y. Wu, Y.-C. Chen, V. Mereacre, A. K. Powell, L. Ungur, L. F. Chibotaru, X.-M. Chen and M.-L. Tong, *Angew. Chem. Int. Ed.*, doi: 10.1002/anie.201407799.

(15) (a) G. Abbas, Y.-H. Lan, V. Mereacre, G. Buth, M. T. Sougrati, F. Grandjean, G. J. Long, C. E. Anson and A. K. Powell, *Inorg. Chem.*, 2013, **52**, 11767; (b) V. Mereacre, F. Klöwer, Y.-H. Lan, R. Clérac, J. A. Wolny, V. Schünemann, C. E. Anson and A. K. Powell, *Beilstein J. Nanotechnol.*, 2013, **4**, 807; (c) F.-H. Zhao, H. Li, Y.-X. Che, J.-M. Zheng, V. Vieru, L. F. Chibotaru, F. Grandjean and G. J. Long, *Inorg. Chem.*, 2014, **53**, 9785.

(16) G.-J. Chen, C.-Y. Gao, J.-L. Tian, J.-K. Tang, W. Gu, X. Liu,S.-P. Yan, D.-Z. Liao and P. Cheng, *Dalton Trans.*, 2011, **40**, 5579.

(17) Y. Bi, Y.-N. Guo, L. Zhao, Y. Guo, S.-Y. Lin, S.-D. Jiang, J.-K. Tang, B.-W. Wang and S. Gao, *Chem.–Eur. J.*, 2011, **17**, 12476.

(18) D.-P. Li, X.-P. Zhang, T.-W. Wang, B.-B. Ma, C.-H. Li, Y.-Z. Li and X.-Z. You, *Chem. Commun.*, 2011, **47**, 6867.

(19) G. Chen, Y. Guo, J. Tian, J.-K. Tang, W. Gu, X. Liu, S. Yan, P. Cheng and D. Liao, *Chem.–Eur. J.*, 2012, **18**, 2484.

(20) Q.-W. Xie, S.-Q. Wu, W.-B. Shi, C.-M. Liu, A.-L. Cui and H.-Z. Kou, *Dalton Trans.*, 2014, **43**, 11309.

(21) H. L. C. Feltham, Y. Lan, F. Klöwer, L. Ungur, L. F. Chibotaru, A. K. Powell and S. Brooker, *Chem.–Eur. J.*, 2011, **17**, 4362.

(22) A. Yamashita, A. Watanabe, S. Akine, T. Nabeshima, M. Nakano, T. Yamamura and T. Kajiwara, *Angew. Chem. Int. Ed.*, 2011, **50**, 4016.

(23) G. Cucinotta, M. Perfetti, J. Luzon, M. Etienne, P. Car, A. Caneschi, G. Calvez, K. Bernot and R. Sessoli, *Angew. Chem. Int. Ed.*, 2012, **51**, 1606.

(24) A. Watanabe, A. Yamashita, M. Nakano, T. Yamamura and T. Kajiwara, *Chem.–Eur. J.*, 2011, **17**, 7428.

(25) Y. Sui, D.-S. Liu, R.-H. Hu and J.-G. Huang, *Inorg. Chim. Acta.*, 2013, **395**, 225.

(26) (a) P. Zhang, L. Zhang, S.-Y. Lin, S.-F. Xue and J.-K. Tang, *Inorg. Chem.*, 2013, **52**, 4587; (b) M. Towatari, K. Nishi, T. Fujinami, N. Matsumoto, Y. Sunatsuki, M. Kojima, N. Mochida, T. Ishida, N. Re and J. Mrozinski, *Inorg. Chem.*, 2013, **52**, 6160; (c) V. Chandrasekhar, S. Das, A. Dey, S. Hossain and J.-P. Sutter, *Inorg. Chem.*, 2013, **52**, 11956; (d) S. Das, S. Hossain, A. Dey, S. Biswas, J.-P. Sutter and V. Chandrasekhar, *Inorg. Chem.*, 2014, **53**, 5020.

(27) E. A. Boudreaux and L. N. Mulay, *In Theory and Application of Molecular Paramagnetism, J.Wiely & Sons*. New York, 1976.

(28) G.M. Sheldrick, *SHELXL-97*, University of Gottingen, Gottingen, Germany, 1997.

(29) (a) M. L. Kahn, R. Ballou, P. Porcher, O. Kahn and J. P. Sutter, *Chem.–Eur. J.*, 2002, **8**, 525; (b) J. D. Rinehart and J. R. Long, *Chem. Sci.*, 2011, **2**, 2078.

(30) L. Kahn, J. P. Sutter, S. Golhen, P. Guionneau, L. Ouahab, O. Kahn and D. Chasseau, *J. Am. Chem. Soc.*, 2000, **122**, 3413.

(31) J.-K. Tang, I. Hewitt, N. T. Madhu, G. Chastanet, W. Wernsdorfer, C. E. Anson, C. Benelli, R. Sessoli and A. K. Powell, *Angew. Chem. Int. Ed.*, 2006, **45**, 1729.

(32) (a) N. Ishikawa, M. Sugita, T. Ishikawa, S. Koshihara and S. J. Kaizu, *Phys. Chem. B*, 2004, **108**, 11265; (b) R. A. Layfield, J. J. W. McDouall, S. A. Sulway, F. Tuna, D. Collison and R. E. P. Winpenny, *Chem.–Eur. J.* 2010, **16**, 4442; (c) M. Jeletic, P.-H. Lin, J. J. Le Roy, I. Korobkov, S. I. Goelsky and M. Murugesu, *J. Am. Chem. Soc.*, 2011, **133**, 19286; (d) P. E. Car, M. Perfetti, M. Mannini, A. Favre, A. Caneschi and R. Sessoli, *Chem. Commun.*, 2011, **47**, 3751; (e) J. Ruiz, A. J. Mota, A. Rodríguez-Diéguez, S. Titos, J. M. Herrera, E. Ruiz, E. Cremades, J. P. Costes and E. Colacio, *Chem. Commun.*, 2012, **48**, 7916.

(33) (a) P.-H. Lin, N. C. Smythe, S. I. Gorelsky, S. Maguire, N. J. Henson, I. Korobkov, B. L. Scott, J. C. Gordon, R. T. Baker and M. Murugesu, *J. Am. Chem. Soc.*, 2011, **133**, 15806; (b) T. Jurca, A. Farghal, P.-H. Lin, I. Korobkov, M. Murugesu and D. S. Richardson, *J. Am.* Chem. *Soc.*, 2011, **133**, 15814; (c) J. Vallejo, I. Castro, R. Ruiz-García, J. Cano, M. Julve, F. Lloret, G. De Munno, W. Wernsdorfer and E. Pardo, *J. Am. Chem. Soc.*, 2012, **134**, 15704.

(34) P. Artus, C. Boskovic, J. Yoo, W. E. Streib, L.-C. Brunel, D. N. Hendrickson and G. Christou, *Inorg. Chem.*, 2001, **40**, 4199.

(35) S. M. J. Aubin, N. R. Dilley, L. Pardi, J. Krzystek, M. W. Wemple, L. C. Brunel, M. B. Maple, G. Christou and D. N. Hendrickson, *J. Am. Chem. Soc.*, 1998, **120**, 4991.

(36) K. S. Cole and R. H. Cole, *J. Chem. Phys.*, 1941**, 9**, 341.

(37) S. M. J. Aubin, Z. M. Sun, L. Pardi, J. Krzystek, K. Folting, L. C. Brunel, A. L. Rheingold, G. Christou and D. N. Hendrickson, *Inorg. Chem.*, 1999**, 38**, 5329.

(38) D. Gatteschi, R. Sessoli and J. Villain, *Molecular Nanomagnets*, Oxford University Press; Oxford, U.K., 2006.

(39) J. Bartolome, G. Filoti, V. Kuncser, G. Schinteie, V. Mereacre, C. E. Anson, A. K. Powell, D. Prodius and C. Turta, *Phys. Rev. B*, 2009, **80**, 014430.

(40) F. Luis, J. Bartolome, J. F. Fernandez, J. Tejada, J. M. Hernandez, X.-X. Zhang and R. Ziolo, *Phys. Rev. B*, 1997, **55**, 11448.

(41) J. Zhu, C.-Z. Wang, F. Luan, T.-Q. Liu, P.-F. Yan and G.-M. Li, *Inorg. Chem.*, 2014, **53**, 8895.

(42) J. Long, F. Habib, P.-H. Lin, I. Korobkov, G. Enright, L. Ungur, W. Wernsdorfer, L. F. Chibotaru and M. Murugesu, *J. Am. Chem. Soc.*, 2011, **133**, 5319; (b) J. D. Rinehart, M. Fang, W. J. Evans and J. R. Long, *J. Am. Chem. Soc.*, 2011, **133**, 14236.

(43) (a) F. Habib, G. Brunet, V. Vieru, I. Korobkov, L. F. Chibotaru and M. Murugesu, *J. Am. Chem. Soc.*, 2013, **135**, 13242; (b) E. M. Pineda, N. F. Chilton, R. Marx, M. Dörfel, D. O. Sells, P. Neugebauer, S.-D. Jiang, D. Collison, J. von Slageren, E. J. L. McInnes and R. E. P. Winpenny, *Nat. Commun.*, 2014, **5**, 5243.